

## **Modelling of Landslides Based on Monitoring Data and the Dynamics of Slopes**

X.L. Ding, Y.Q. Chen, J.J. Zhu  
Department of Land Surveying and  
Geo-Informatics

K.T. Chau  
Department of Civil and Structural  
Engineering

Hong Kong Polytechnic University, Hung Hom, Kowloon, Hong Kong  
Telephone: +852 2766 5965/5966; Fax: +852 2330 2994; Email: lsxlding/lisyqchen@polyu.edu.hk

### **ABSTRACT**

It is a common practice nowadays to monitor the progressive deformations of potentially dangerous slopes to avoid the damages caused by unexpected landslides. However, simple geometrical approaches are mainly used for the analysis of slope monitoring data. While such approaches can reflect to certain extent the general behaviour of the monitored slopes, it is often difficult to use them alone to understand the deformation/failure mechanism of a slope and to make reliable prediction of landslide.

This paper describes a method of modelling landslides based on both deformation monitoring data and the dynamics of slopes. Based on the assumption that a slope consists of rigid blocks, the dynamic models of the slope are established. The models are then used as system equations in a Kalman filter model. The approach is more advantageous in principle than purely studying monitoring data or the dynamics of a slope. Both the concept and results from numerical examples are presented.

### **1. Introduction**

Slopes, either natural mountain slopes or slopes that are formed as a result of constructions or open pit mining, can lead to landslides under certain conditions. Unexpected landslides can often cause catastrophes resulting in loss of lives and facilities such as roads and buildings. It is a common practice nowadays to monitor the progressive deformations of potentially dangerous slopes to avoid or to reduce the damages caused by unexpected landslides.

Simple approaches are however usually used to analyse slope monitoring data. For example, the data are often fitted into straight lines or curves to detect the trend of deformations. Although such approaches can help to understand to certain extent the general behaviour of the monitored slopes, they are not rigorous, unable to fully utilise the information contained in the data, and hardly able to tell the state of stability of the monitored slopes. Besides, purely looking at monitoring data without taking into consideration of the deformation and failure mechanisms and the mechanical properties of a slope may even lead to misleading results.

This paper describes a method of modelling landslides based on both deformation monitoring data and the dynamics of slopes. The two are combined through the use of a Kalman filter model. The

approach is more advantageous in principle than purely studying monitoring data or the dynamics of a slope. Both the concept and results from numerical examples are presented.

## 2. The Dynamic Model of Slopes

A slope fails typically in plane, wedge, curve or toppling mode (e.g., Hoek and Bray 1981; Craig, 1983). We will however limit our discussions in this paper to slopes that consist of sliding rigid body blocks (Fig. 1) (e.g., Shi, 1988).

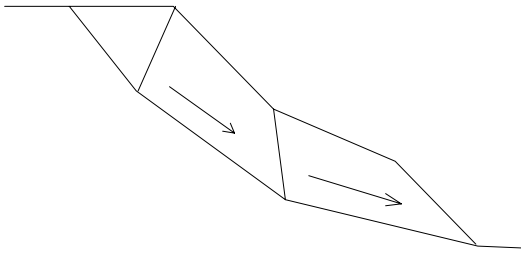


Figure 1: Block failure system

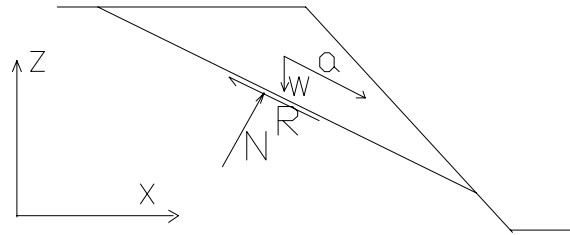


Figure 2: A sliding block on a plane

If the geometry and material properties (e.g., coefficient of friction and unit weight) of a block system are known, the motion of the system can be derived. From Newton's second law of motion, the displacement of any block in a block system can be described by (Fig. 3):

$$\begin{aligned} m_i a_{ix} &= N_{ix} + R_{ix} + P_{i,i-1x} + P_{i,i+1x} + T_{i,i-1x} + T_{i,i+1x} \\ m_i a_{iz} &= N_{iz} + R_{iz} + P_{i,i-1z} + P_{i,i+1z} + T_{i,i-1z} + T_{i,i+1z} - m_i g \end{aligned} \quad (2)$$

where  $a_x$ ,  $a_z$  are accelerations of the mass centre of the  $i$ th sliding block, that is

$$a_{ix} = \frac{\partial^2 x_i}{\partial t^2}, \quad a_{iz} = \frac{\partial^2 z_i}{\partial t^2}; \quad (3)$$

$N$  is the normal force exerted on the surface of the block by the stable bed rock of the slope;  $R$  is the resistant force as a result of frictions;  $N_x$ ,  $N_z$ ,  $R_x$ ,  $R_z$  are the elements of  $N$  and  $R$  in the  $x$  and  $z$  directions, respectively;  $m$  is the mass of the block;  $g$  is the acceleration due to gravity;  $x_i$ ,  $z_i$  are the displacements of the block;  $P$  and  $T$  are the corresponding forces from the adjacent blocks; and  $t$  is the time. Equation (2) can also be written as

$$M_i a_i = A_i Y_i + F_i \quad (4)$$

where

$$A_i = \begin{pmatrix} \sin \alpha_i & -\cos \alpha_i & \sin \beta_{i,i-1} & -\sin \beta_{i,i+1} & -\cos \beta_{i,i-1} & \cos \beta_{i,i+1} \\ \cos \alpha_i & \sin \alpha_i & -\cos \beta_{i,i-1} & \cos \beta_{i,i+1} & -\sin \beta_{i,i-1} & \sin \beta_{i,i+1} \end{pmatrix}$$

$$Y_i = (N_i \quad R_i \quad P_{i-1,i} \quad P_{i,i+1} \quad T_{i-1,i} \quad T_{i,i+1})$$

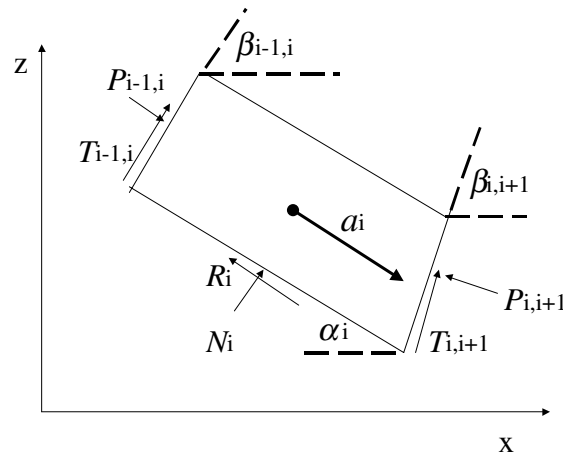


Figure 3: The geometry and forces associated with a rigid block

$$M_i = \begin{pmatrix} m_i & 0 \\ 0 & m_i \end{pmatrix}$$

$$a_i = (a_{xi} \quad a_{zi})$$

For the entire system of blocks, a general equation of the form of (4) can be formed

$$Ma = A_1 Y + G \quad (5)$$

where

$$Y = (N_1, N_2, \dots, N_i, \dots, R_1, \dots, R_i, \dots, P_{1,2}, \dots, P_{i,i+1}, \dots, P_{n-1,n}, T_{1,2}, \dots, T_{i,i+1}, \dots, T_{n-1,n})^T$$

$$a = (a_{x1}, a_{z1}, \dots, a_{xi}, a_{zi}, \dots, a_{xn}, a_{zn})^T$$

$$G = (0, m_1 g, \dots, 0, m_i g, \dots, 0, m_n g)^T$$

$M$  and  $A_1$  are formed according to  $M_i$  and  $A_{1i}$  respectively. Equation (5) describes the motion of a system of rigid body blocks. Obviously, if only one block is considered, then

$$Y = \begin{pmatrix} N \\ R \end{pmatrix} \quad G = \begin{pmatrix} 0 \\ mg \end{pmatrix} \quad A_1 = \begin{pmatrix} \sin \alpha & -\cos \alpha \\ \cos \alpha & \sin \alpha \end{pmatrix} \quad (6)$$

Under the assumption of rigidity of the blocks and the constraints of the geometry, any block can only move along the surfaces of discontinuities. This means that for any block, there must exist,

$$a_{xi} \tan \alpha_i + a_{zi} = 0 \quad (7)$$

If there are  $n$  blocks in the system, there must be  $n$  such equations.

Besides, the displacements, velocities and accelerations of two adjacent blocks are assumed the same in directions normal to the surfaces of discontinuity. Therefore, for acceleration, there exists

$$a_{xi} \sin \alpha_{i,i+1} - a_{zi} \cos \alpha_{i,i+1} = a_{xi+1} \sin \alpha_{i,i+1} - a_{zi+1} \cos \alpha_{i,i+1} \quad (8)$$

If there are  $n$  blocks in the system, there must exist  $n-1$  such equations. For the block system, Equation (7) and (8) can be combined into:

$$A_2 a = 0 \quad (9)$$

where  $A_2$  can be formed according to (7) and (8).

The friction forces depend on the normal forces, i.e.,

$$\begin{aligned} R_i &= kN_i + c \\ T_i &= kP_i + c \end{aligned} \quad (10)$$

where  $k$  is the coefficient of friction; and  $c$  is the force of cohesion. For a system of  $n$  blocks, there must exist  $2n-1$  such equations. The equations can be expressed as

$$A_3 Y = C \quad (11)$$

Finally, the equations in (5), (9) and (11) can be expressed as

$$AX = L \quad (12)$$

where

$$A = \begin{pmatrix} -M & A_1 \\ A_2 & 0 \\ 0 & A_3 \end{pmatrix}, \quad L = \begin{pmatrix} -G \\ 0 \\ C \end{pmatrix}, \quad X = \begin{pmatrix} a \\ Y \end{pmatrix}$$

There are in (12)  $6n-2$  unknowns and  $6n-2$  equations. Therefore the equations have a unique solution. Multiplying Equation (12) by  $A^T$ , one gets

$$A^T AX = A^T L \quad (13)$$

and

$$X = (A^T A)^{-1} A^T L \quad (14)$$

After the accelerations are found from the above, one can derive the motion of the slope using:

$$V_{xi} = \frac{\partial X_i}{\partial t} = \int a_{xi} dt, \quad V_{zi} = \frac{\partial Z_i}{\partial t} = \int a_{zi} dt \quad (15a)$$

$$X_i = \iint a_{xi} dt dt, \quad Z_i = \iint a_{zi} dt dt \quad (15b)$$

In a small time step, one can get:

$$\begin{aligned} V_{xi} &= V_{xio} + a_{xi}t, & V_{zi} &= V_{zio} + a_{zi}t \\ X_i &= X_{i0} + V_{xi0}t + \frac{1}{2}t^2a_{xi}, & X_i &= X_{i0} + V_{xi0}t + \frac{1}{2}t^2a_{xi} \end{aligned} \quad (16)$$

Equations (12), (15) and (16) constitute the forward model of the slope. Based on the known geometry and material properties, one can find the displacement of the slope.

If Equation (12) is used directly, double precision variables are needed to use in programming since most numbers need at least 16 digits. In order to improve the computation accuracy and make the numerical computation more stable, we make a transformation of parameters  $Y$ . Let

$$Y = Y_0 + \Delta Y$$

where  $Y_0$  is the value of  $Y$  when in the state of limiting equilibrium. Since the acceleration of any slope body will be  $a_{xi}=a_{zi}=0$  in an equilibrium state, from (5) and (11), one can get

$$\begin{aligned} A_1 Y_0 + G_0 &= 0 \\ A_3 Y_0 &= C_0 \end{aligned} \quad (17)$$

$G_0$ ,  $C_0$  is the values of  $G$  and  $C$  in the limiting equilibrium state. Substituting (17) into (12), the equation becomes

$$\begin{pmatrix} -M & A_1 \\ A_2 & 0 \\ 0 & A_3 \end{pmatrix} \begin{pmatrix} a \\ \Delta Y \end{pmatrix} = \begin{pmatrix} -\Delta G \\ 0 \\ \Delta C \end{pmatrix} \quad (18)$$

where

$$\begin{aligned} \Delta Y &= Y - Y_0, & \Delta C &= C - C_0 \\ \Delta G &= G - G_0 = (0, \Delta m_1 g, \dots, 0, \Delta m_i g, \dots) \end{aligned}$$

In order to keep symbols simple, we will still use

$$X = \begin{pmatrix} a \\ \Delta Y \end{pmatrix}, \quad L = \begin{pmatrix} -\Delta G \\ 0 \\ \Delta C \end{pmatrix}$$

in the rest of the paper. Equation (18) can still be written as

$$AX = L \quad (19)$$

It is obvious that  $\Delta Y$  describes the difference between the present state and the stable state.

### 3 Kalman Filter Model

The state of a sliding slope can be described by the following state vector,

$$X = (X_1^T, V^T, a^T, \Delta Y^T)^T \quad (20)$$

where

$$\begin{aligned} X_1 &= (x_1, z_1, \dots, x_i, z_i, \dots)^T \\ V &= \dot{X}_1 = (v_{x1}, v_{z1}, \dots, v_{xi}, v_{zi}, \dots)^T \\ a &= \dot{V} = (a_{x1}, a_{z1}, \dots, a_{xi}, a_{zi}, \dots)^T \end{aligned}$$

$X_1$  is the vector of displacements,  $V$  is the vector of velocities.

Four different state transition models can be derived:

(1). The first one is based on the rigid body motion equation and on the forward analysis model. According to the rigid body motion equation, when the state transits from state  $k$  to state  $k+1$ , the displacement and the velocity will change to:

$$\begin{aligned} X_{1,k+1} &= X_{1,k} + tV_k + \frac{1}{2}t^2 a_k \\ V_{1,k+1} &= V_k + ta_k \end{aligned} \quad (21)$$

In real situations, the external forces acting on a slope body usually will not change except when for example the ground water level changes after rains. Therefore it is reasonable to assume  $\Delta G=0$  and  $\Delta Y_{k+1}=\Delta Y_k$ . If there exist any changes in the external forces, they can be considered as state transition errors (system noises) if the changes are not very significant. Based on this assumption and Equation (18), one can get:

$$\begin{aligned} \Delta Y_{k+1} &= \Delta Y_k \\ a_{k+1} &= M^{-1}A_1\Delta Y_{k+1} + M^{-1}\Delta G = M^{-1}A_1\Delta Y_k \end{aligned} \quad (22)$$

Combining (21) with (22), we can get the following state transition equation:

$$X_{k+1} = \Phi_k X_k = \begin{pmatrix} I & tI & \frac{1}{2}t^2 & 0 \\ 0 & I & t & 0 \\ 0 & 0 & 0 & M^{-1}A_1 \\ 0 & 0 & 0 & I \end{pmatrix} \begin{pmatrix} X_{1,k} \\ V_k \\ a_k \\ \Delta Y_k \end{pmatrix} \quad (23)$$

(2). The second state transition model is based on the forward analysis model only. The time-dependent state equation is

$$\dot{X} = \begin{pmatrix} \dot{X}_1 \\ \dot{V} \\ \dot{a} \\ \dot{\Delta Y} \end{pmatrix} = \begin{pmatrix} V \\ a \\ 0 \\ 0 \end{pmatrix} = \begin{pmatrix} V \\ M^{-1}A_1\Delta Y + \Delta G \\ 0 \\ 0 \end{pmatrix} = \begin{pmatrix} 0 & I & 0 & 0 \\ 0 & 0 & 0 & M^{-1}A_1 \\ 0 & 0 & 0 & 0 \\ 0 & 0 & 0 & 0 \end{pmatrix} \begin{pmatrix} X_1 \\ V \\ a \\ \Delta Y \end{pmatrix} \quad (24)$$

where

$$\dot{X} = \frac{\partial X}{\partial t}, \quad \dot{X}_1 = \frac{\partial X_1}{\partial t}, \quad \dot{a} = \frac{\partial a}{\partial t}, \quad \Delta \dot{Y} = \frac{\partial \Delta Y}{\partial t}, \quad \Delta G = 0$$

By discretising the above continuous-time state equation using series expansions (e.g., Ren and Ding., 1996), a discrete-time state equation is obtained:

$$X_{k+1} = \Phi_k X_k = \begin{pmatrix} I & tI & 0 & \frac{1}{2}t^2M^{-1}A_1 \\ 0 & I & 0 & tM^{-1}A_1 \\ 0 & 0 & I & 0 \\ 0 & 0 & 0 & I \end{pmatrix} \begin{pmatrix} X_{1,k} \\ V_k \\ a_k \\ \Delta Y_k \end{pmatrix} \quad (25)$$

(3). The third model is an improved form of the second. The model given in (25) above can be substituted by

$$X_{k+1} = \Phi_k X_k = \begin{pmatrix} I & tI & \frac{1}{2}t^2M^{-1}A_1 \\ 0 & I & tM^{-1}A_1 \\ 0 & 0 & I \end{pmatrix} \begin{pmatrix} X_{1,k} \\ V_k \\ \Delta Y_k \end{pmatrix} \quad (26)$$

that is, in this model

$$X = \begin{pmatrix} X_1 \\ V \\ \Delta Y \end{pmatrix}$$

This means that the third model is the same as the second, but has less parameters in the state vector. The model is therefore simpler.

(4). The last model is the one widely used in kinematic systems. In this model, only the rigid motion equation is considered (e.g., Chui, 1987),

$$X_{k+1} = \Phi_k X_k = \begin{pmatrix} I & tI & \frac{1}{2}t^2 \\ 0 & I & t \\ 0 & 0 & I \end{pmatrix} \begin{pmatrix} X_{1,k} \\ V_k \\ a_k \end{pmatrix} \quad (27)$$

The stochastic state transition equation is obtained if the state transition errors (the system noises)  $w$  are added to (23), (25) or (26):

$$X_{k+1} = \Phi_k X_k + w. \quad (28)$$

In slope deformation monitoring, observation equations can be established for all the observations,

$$L_1 = B_1 X + \varepsilon_1 \quad (29)$$

where

$$B_1 = \begin{pmatrix} I & 0 & 0 \end{pmatrix}$$

Under the assumption that the slope bodies are rigid, one can establish some constraints. For example, according to the forward model (18), we have,

$$\begin{aligned} A_2 a_{k+1} &= 0 \\ A_3 \Delta Y_{k+1} &= \Delta C \end{aligned} \quad (30)$$

These can be used as geometric constraints. Besides, the displacements and velocities of the two blocks that are adjacent to each other must be the same in the normal direction of the contact surface. Therefore, similar to Equation (9), the following should hold,

$$\begin{aligned} A_2 X_{1,k+1} &= 0 \\ A_2 V_{k+1} &= 0 \end{aligned} \quad (31)$$

(30) and (31) can be rewritten as

$$B_2 X_{k+1} = L_2 \quad (32)$$

where

$$B_2 = \begin{pmatrix} A_2 & 0 & 0 & 0 \\ 0 & A_2 & 0 & 0 \\ 0 & 0 & A_2 & 0 \\ 0 & 0 & 0 & A_3 \end{pmatrix}, \quad L_2 = \begin{pmatrix} 0 \\ 0 \\ 0 \\ \Delta C \end{pmatrix}$$

In the real situations, Equation (32) may not be completely satisfied due to reasons such as the errors in the assumptions. For example, the blocks will always more or less deform and therefore are not exactly rigid. Besides, the failure surfaces may also be known only approximately. One better way to treat the constraints is to consider them as observations with certain uncertainties,

$$B_2 X_{k+1} = L_2 + \varepsilon_2 \quad (33)$$

where  $\varepsilon_2$  is an error term. The above equations can be used as observation equations.

Based on (24), (25) and (30), we can get the following Kalman filter model

$$X_{k+1} = \Phi_k X_k + w \quad (34)$$

$$L_{k+1} = B X_{k+1} + \varepsilon, \quad P_{k+1} \quad (35)$$

$$B = \begin{pmatrix} B_1 \\ B_2 \end{pmatrix}, \quad L_{k+1} = \begin{pmatrix} L_{1,k+1} \\ L_2 \end{pmatrix}, \quad P_{k+1} = \begin{pmatrix} P_L & 0 \\ 0 & P_{\varepsilon_2} \end{pmatrix}$$

The computation formulae of Kalman filter are (e.g., Chui, 1987):



$$\begin{aligned}
 \bar{X}_{k+1} &= \Phi_k \hat{X}_k \\
 Q_{\bar{X}_{k+1}} &= \Phi_k Q_{\hat{X}_k} \Phi_k^T + Q_w \\
 \hat{X}_{k+1} &= \bar{X}_{k+1} + Q_{\bar{X}_{k+1}} B^T (B Q_{\bar{X}_{k+1}} B^T + Q_{k+1})^{-1} (L_{k+1} - B \bar{X}_{k+1}) \\
 Q_{\hat{X}_{k+1}} &= Q_{\bar{X}_{k+1}} - Q_{\bar{X}_{k+1}} B^T (B Q_{\bar{X}_{k+1}} B^T + Q_{k+1})^{-1} B Q_{\bar{X}_{k+1}}
 \end{aligned} \tag{36}$$

or (e.g., Jia et al, 1998)

$$\begin{aligned}
 \hat{X}_{k+1} &= \bar{X}_{k+1} + J (L_k - B \bar{X}_{k+1}) \\
 Q_{\hat{X}_{k+1}} &= (I - JB) Q_{\bar{X}_{k+1}} \\
 J &= Q_{\bar{X}_{k+1}} B^T (B Q_{\bar{X}_{k+1}} B^T + Q_{k+1})^{-1}
 \end{aligned} \tag{37}$$

where

$$Q_{k+1} = P_{k+1}^{-1}, \quad Q_w = P_w^{-1}$$

In practical computations, two problems must be considered when the above formulae are used, i.e., the initial values of  $X$ , and the variances of the system errors  $w$  and the model errors  $\varepsilon_2$  (or the model uncertainty). The initial values of  $X$  can be determined by using the condition of limiting equilibrium. If a slope has already begun to slide, the displacements, velocities and the accelerations can be determined by using initial two epochs of surveys.

## 5 Numerical Esxamples

Simulated examples are given here to show the feasibility of the Kalman filter model presented above. The block system used in the simulated examples is similar to that shown in Fig. 5. The parameters of the system are taken as,  $m_1=798000$  kg,  $m_2=4000000$  kg,  $m_3=400000$  kg,  $\alpha_1=60$ ,  $\alpha_2=45$ ,  $\alpha_3=30$ ,  $\alpha_{12}=60$  and  $\alpha_{23}=75$ , and the cohesion force  $c=0$ . The coefficient of friction  $k$  in the state of limiting equilibrium is  $k=0.7670573627281236$ . One observed point was placed on each of the three blocks, and observations of the horizontal and vertical displacements of the observed points were simulated. The observations were taken once every 5 days for one year period. The variance of the simulaed errors is  $\sigma^2 = 3^2$  mm<sup>2</sup>.

After the observations were taken, the Kalman filer model (23), (25), (26) and (27) were used respectively to process the data. Figs. 8, 9,10 and 11 give the results from the different models. In these figures, the simulated observations, the real displacements and values computed by the Kalman filter are given. Table 2 lists the following values for each of the Kalman filter models,

$$\begin{aligned}
 \delta_\Sigma &= \sum (\hat{x}_k - \bar{x}_k)^2 \\
 \sigma_k &= \sqrt{\frac{\delta_\Sigma}{n}}
 \end{aligned} \tag{38}$$

where  $\hat{x}_k$  and  $\bar{x}_k$  are the filtered and the true (simulated) displacements respectively, and  $n$  is the number of epoches.

Table 2. Filtering deviations (38)

		$X_1$	$Z_1$	$X_2$	$Z_2$	$X_3$	$Z_3$
Model (1)	$\delta_{\Sigma}$	35.06	105.15	56.32	56.34	67.93	22.68
	$\sigma_k$	0.708	1.226	0.897	0.897	0.985	0.569
Model (2)	$\delta_{\Sigma}$	33.40	100.16	53.66	53.68	64.71	21.60
	$\sigma_k$	0.691	1.196	0.876	0.876	0.962	0.556
Model (3)	$\delta_{\Sigma}$	33.40	100.16	53.66	53.68	64.71	21.60
	$\sigma_k$	0.691	1.196	0.876	0.876	0.962	0.556
Model (4)	$\delta_{\Sigma}$	242.23	338.58	502.48	354.28	317.60	383.48
	$\sigma_k$	1.860	2.199	2.679	2.250	2.130	2.341

It can be seen from Table 2 and the diagrams:

- (1) The results from the first three models are much more accurate than the original observed values. The variances decreased by 6 ( $3^2/1.226^2$ ) to 29 ( $3^2/0.556^2$ ) times.
- (2) The results from (25) are the same as those from (26). This means that the two models are equivalent, but the computations using (26) are simpler. The results from both (25) and (26) are better than those from (23).
- (3) The results from (23), (25) and (26) are all significantly better than those from (27). This means that the Kalman filter based on the mechanical model of the slope is significantly better.

## 6 Conclusions

- (1) Under the assumption that the slope bodies are rigid, the dynamic models of a sliding slope have been derived. If the required mechanical parameters are known, the dynamic process of the slope can be derived from the models.
- (2) The dynamic models of the sliding slopes are used as system equations in a Kalman filter mode. The dynamical properties of a slope are thus combined with deformation monitoring data through the use of the Kalman filter model.
- (3) The uncertainty in the mechanical properties of a slope or model errors are taken into consideration by using additional fictitious observation equations.
- (4) As the mechanical properties of slopes vary considerably from one to another, further research is still required to take into account the special characteristics of the various types of slopes.

## Acknowledgements

The research was supported by a grant from the Research Grants Council of the Hong Kong Special Administrative Region (Project No. PolyU 5051/98E) and the National Natural Science Foundation of China (program No.49774209).

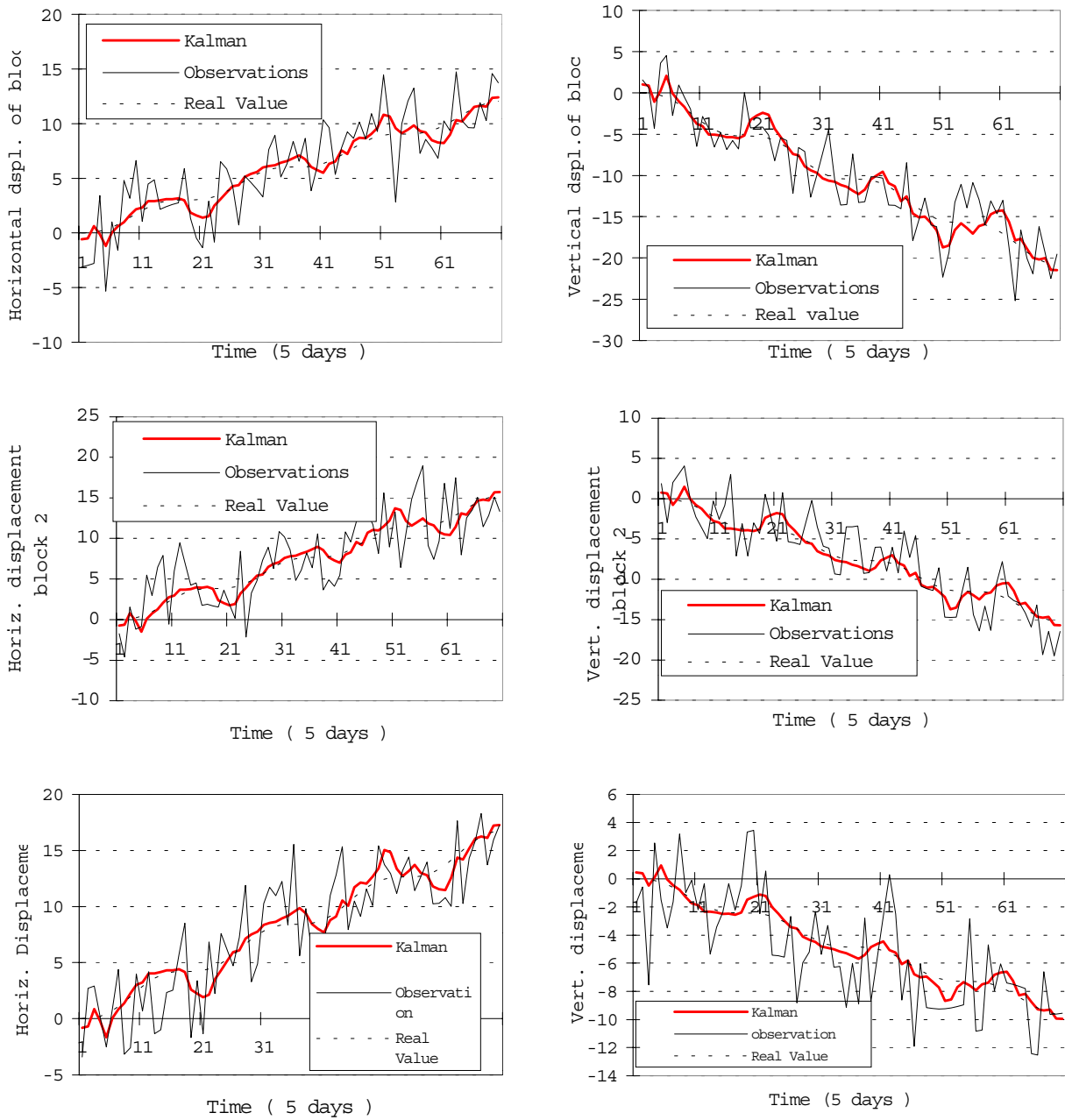


Figure 4: The displacement curve from Model 1

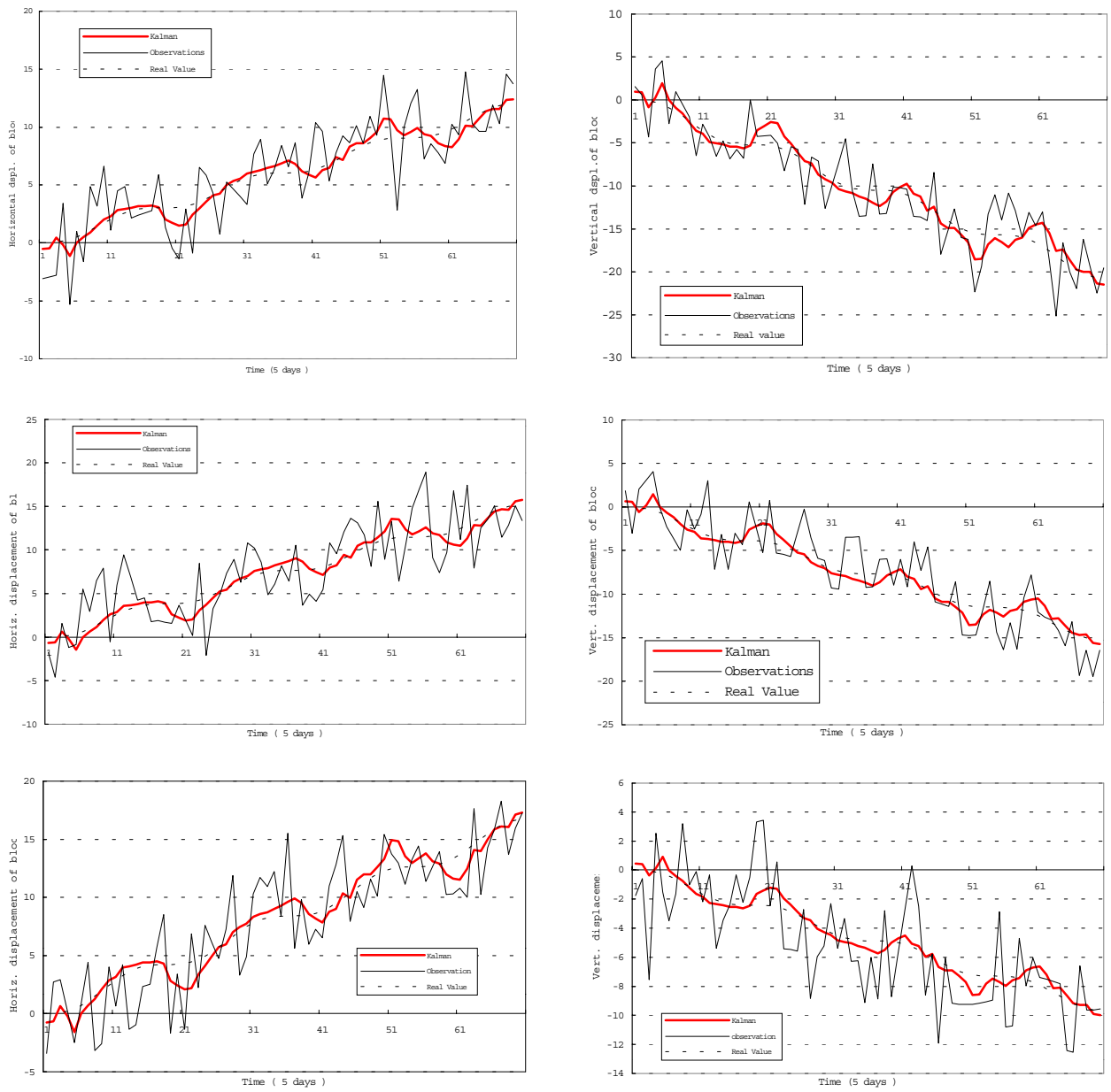


Figure 5: The displacement curve from Model 2

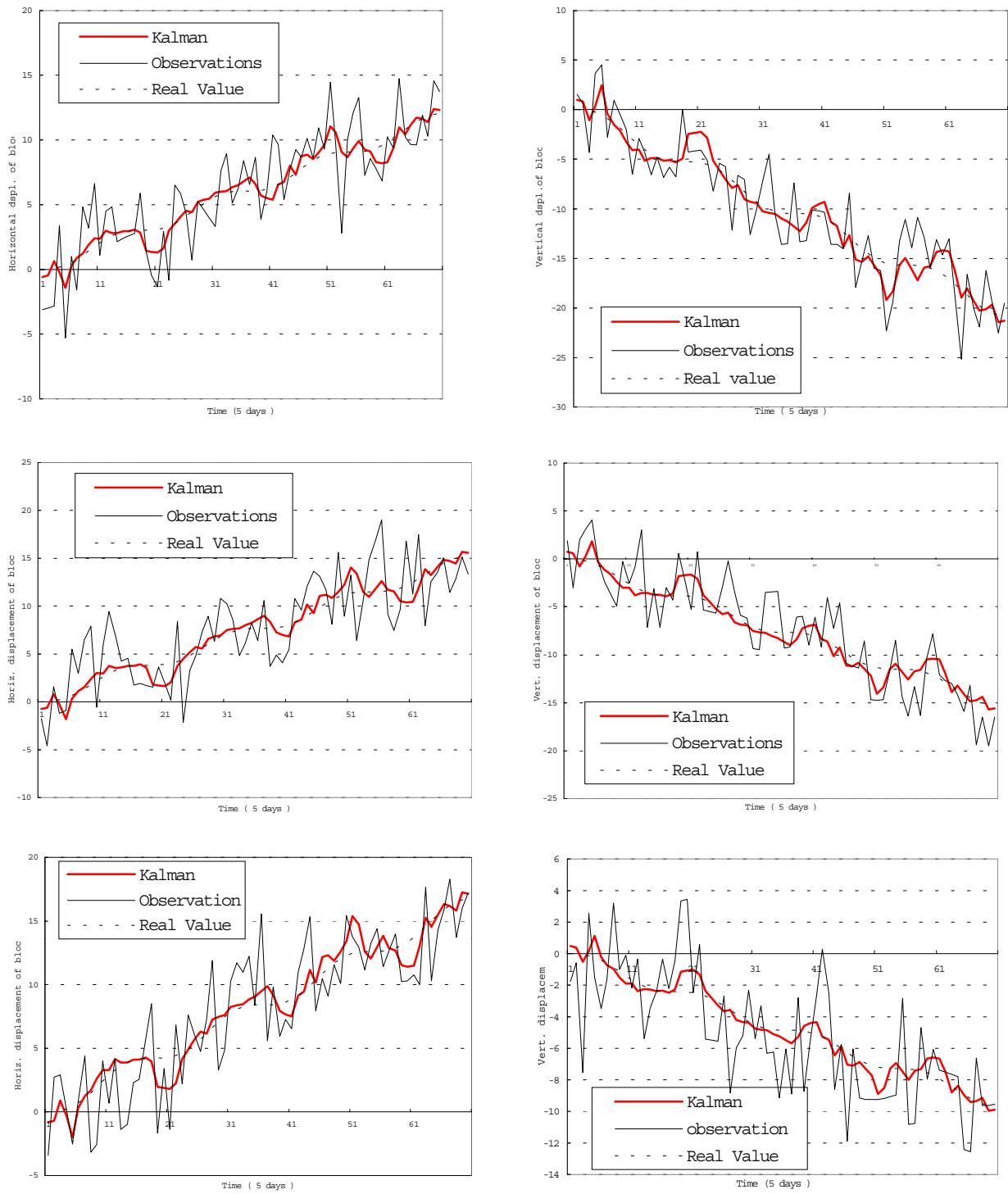


Figure 6: The displacement curve from Model 3

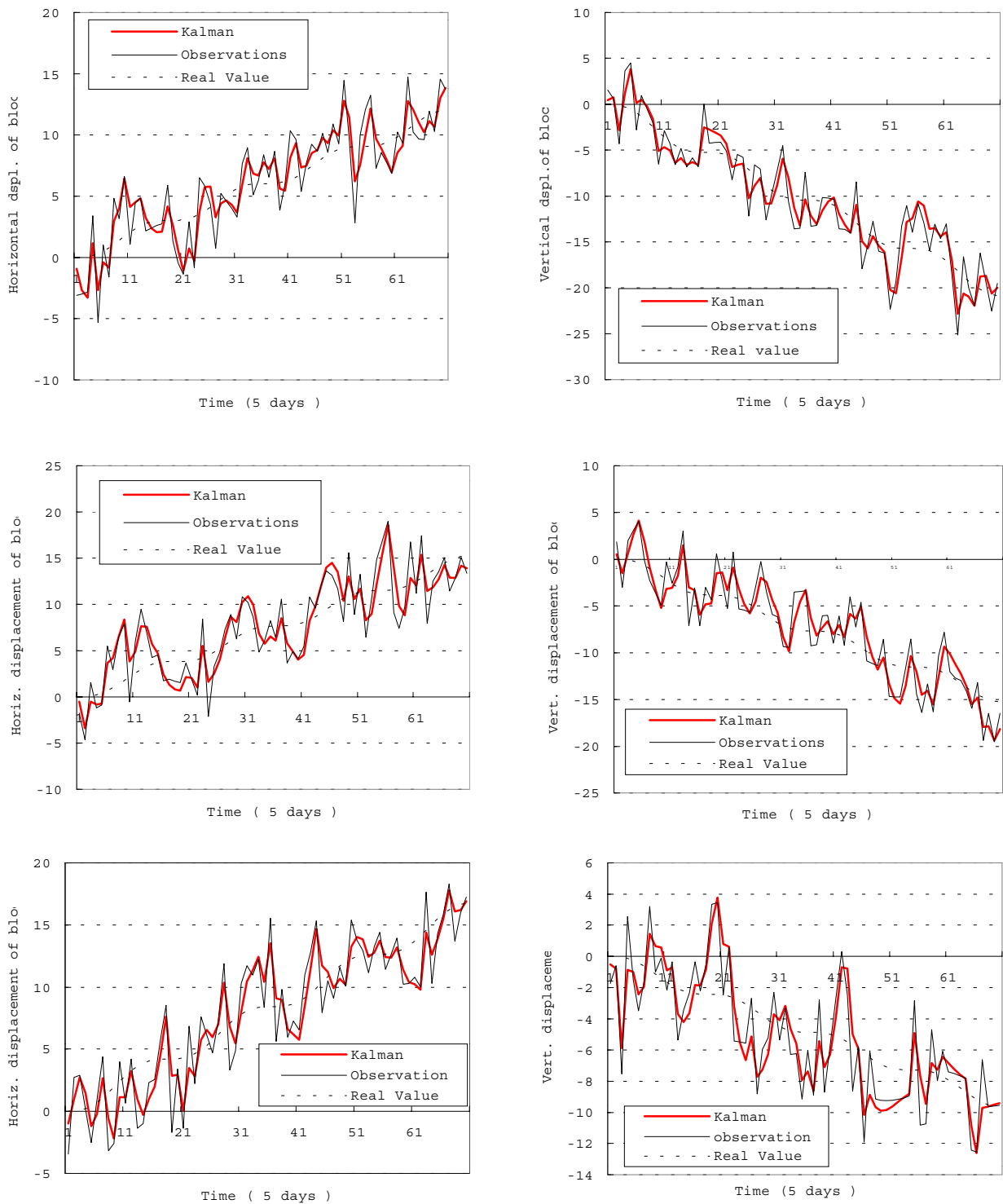


Figure 7: The displacement curve from Model 4

**References**

Chui, C.K. and Chen, G. (1992) Kalman Filtering with Real-Time applications, Springer-Verlag, Berlin, New York.  
 Craig, R.F. (1983) Soil mechanics, Van Nostrand Reinhold (UK) Co.Ltd. Molly Millars Lane, Wokingham, Berkshire, England.

- Hoek, E. and Bray, J.W. (1981) Rock slope engineering, the institution of mining and Metallurgy, London
- Jia, M. and Ding, X., and Montgomery, B., (1998) On reliability measures for kinematic surveys, Geomatica, Vol. 52, No.1, pp.37-44.
- Ren, D. and Ding, X. (1996) Dynamic Deformation Analysis of open pit slopes, The 8<sup>th</sup> Fig International symposium on deformation measurements. 25-28 June 1996, HongKong, pp. 157-163
- Shi, G.H. (1993), Block System Modelling by Discontinuous Deformation analysis, Computational Mechanics Publications, Southampton UK and Boston USA